Non-stationary shear wave statics in the radial trace domain

Raul Cova, David Henley and Kris Innanen

ABSTRACT

Shear-wave statics are one of the main problems in converted-wave processing. The lack of a good correlation between P- and S-wave velocities in the near surface introduces a whole new problem to be solved. Due to its very low velocity values the magnitude of the S-wave statics are several times larger than the P-wave statics, producing a very destructive effect when stacking traces. In this paper it is shown how S-wave statics may also show a non-stationary behaviour. This effect was studied in terms of variations in the transmission angle through the low velocity layer (LVL) due to changes in offset and as a result of the structure of the LVL. An analytic expression for computing deviated travel times through the LVL in terms of its dip, thickness and velocity is proposed here. This expression may be used as the engine for an iterative non-linear inversion algorithm that will allow us to compute velocity models for the near surface given a set of delay times and the ray-path angles associated with them.

INTRODUCTION

Solving statics problems is one of the most important steps in processing seismic data. Statics can introduce undesired effects which may deteriorate vertical resolution, stacking power or even introduce false structures in the seismic section. These problems are present when processing either P- or PS-wave data. However, due to the low velocity of S-waves in the near surface, S-wave statics can be several times larger than P-wave statics. Furthermore, interaction of the S-waves with the near surface may be different than that for P-waves. The location of the water table is one of the features which impacts the velocity of P-waves in an important way. However, since the velocity of S-waves is not affected by the presence of fluids in the rocks, the structure of the near surface "seen" by S-waves may differ from the one affecting P-waves. All these features make the computation of S-wave statics a very complex problem.

Conventionally, near surface statics, either for P- or S- waves, are addressed by assuming surface consistency and stationarity in the behaviour of the delay times. Henley (2012) explains how these concepts start to fail when the velocity of the near surface is higher than the underlying medium (e.g. permafrost, surface carbonates) or when large lateral changes of velocity may lead to multi-path arrivals. In this work we study the change in static times due to variations on the angle of propagation of the wavefield through the low velocity layer (LVL). By using ray-tracing and finite-difference modelling we show how the near surface statics may become a non-stationary problem. Both the effect of velocities and the geometry of the LVL are addressed in order to achieve an analytical expression for modelling ray-path dependent travel times. Although it is not part of this study, this will allow us to develop a new method for computing near surface velocity models by solving ray-path dependent statics.

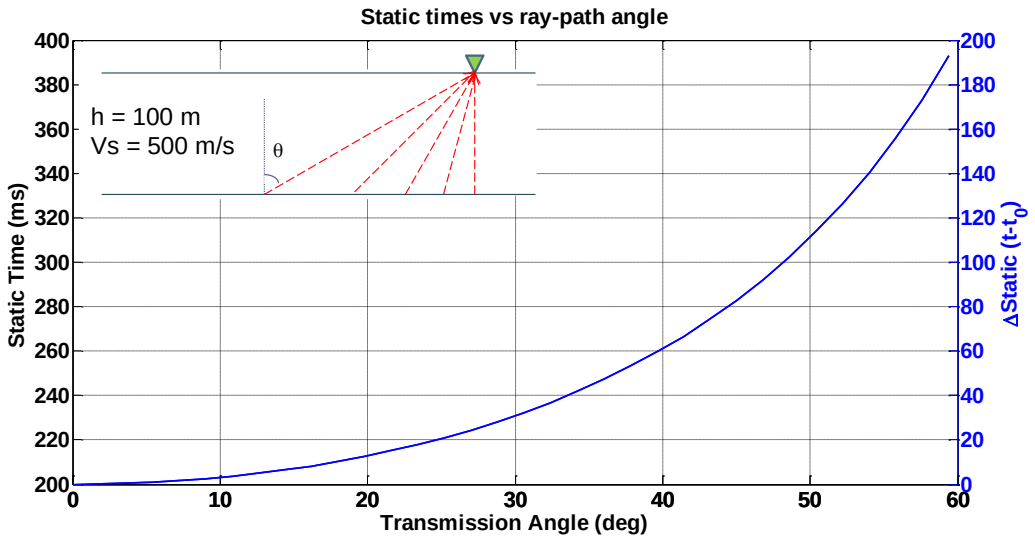

FIG. 1. Static time vs. angle of transmission for a 100 m thickness LVL and S-wave velocity V_s=500 m/s

S-wave static non-Stationarity

Most of the traditional approaches for statics solution rely on the assumption of nearly-vertical ray-paths through the LVL responsible for statics. However, the low velocity of S-waves magnifies the delays in travel time produced by the violation of the vertical-raypath assumption. Figure 1 shows the expected variations in travel time through a LVL with 100 m thickness and S-wave velocity V_s=500 m/s. For that model the vertical ray-path travel time is 200 ms. However, for a wavefront arriving with a deviation of 30° it may have an additional 30 ms delay. This delay is in the same order of magnitude as P-wave refraction statics. Hence, we need to correct this delay before stacking the seismic traces.

Based on Snell's law it is possible to compute the transmission angle of a wavefield propagating through the LVL. As in equation 1, the transmission angle (ϕ_{LVL}), of an up-coming wavefield with incident angle (ϕ_1) depends on the velocity ratio between both media. It is important to note that both angles are relative to the normal defined by the interface.

$$\frac{\sin(\phi_1)}{v_1} = \frac{\sin(\phi_{LVL})}{v_{LVL}}. \tag{1}$$

Solving equation 1 for $\sin(\phi_{LVL})$,

$$sin\phi_{LVL} = \frac{v_{LVL}}{v_1} sin\phi_1, \tag{2}$$

Equation 2 can be used for understanding the effect of the velocity contrast on the transmission angle. When $v_{LVL} \ll v_1$, the ratio $v_{LVL}/v_1 \approx 0$, and regardless of the magnitude of the incidence angle ϕ_1 the transmission angle ϕ_{LVL} will be close to zero. This is the basic condition which supports the assumption of vertical ray-paths through the

LVL. However, when the ratio $v_{LVL}/v_1 \approx 1$, the transmission angle will have a magnitude close to that of the incidence angle. Therefore, we can state that the velocity ratio v_{LVL}/v_1 has the effect of constraining the range of angles in which a wavefield may be transmitted.

The vertical travel time t_0 through the LVL can be written as,

$$t_0 = \frac{h}{v_{LVL}}, \tag{3}$$

where h is the vertical thickness of the LVL. Additionally, the travel time at any given transmission angle ϕ_{LVL} can be computed as,

$$t = \frac{h}{v_{LVL}} \frac{1}{\cos(\phi_{LVL})}. \tag{4}$$

Then, the difference $t - t_0$ is,

$$t - t_0 = \frac{h}{v_{LVL}} \left(\frac{1}{\cos(\phi_{LVL})} - 1 \right). \tag{5}$$

Figure 2 shows the maximum expected transmission angle for a range of velocity ratios from 0 to 1 and the maximum static change as predicted by equation 5 . There we can notice that for velocity ratios less than 0.3 the deviation from the vertical travel time is less than 10 ms. This magnitude is close to the upper limit of what can be considered as a residual static. However, for ratios larger than 0.4, static changes may be of more than 20 ms and may reach more than 100 ms if the velocity of the LVL is close to the velocity of the underlying medium. Hence, smooth changes in velocities in the LVL may lead to large variations in the static value depending on the transmission angle.

One additional degree of complexity can be introduced if we consider that the base of the LVL has some dip. In this case, the deviation from the vertical ray-path assumption is not just controlled by the velocity ratio but also by the dip of the LVL. Figure 3 shows the geometry of the problem.

The travel time along the solid ray depicted in Figure 3 can be computed using the following expression:

$$t = \frac{h}{v_{LVL}} \frac{\cos(\theta)}{\cos(\phi_{LVL} - \theta)}. \tag{6}$$

where θ is the dip angle of the base of the LVL.

It is important to note that when the dip angle θ is set to zero, equation 6 is reduced to equation 4.

In Figure 4 we can see the combined effect of the dip of the LVL and the variation of the ray-path angles on the computation of travel times as predicted by equation 6. The zone in which the deviation of the vertical travel times versus deviated travel times is less than 10 ms can be considered as a safe zone since this delay falls into the order of magnitude of the residual statics. However, for dip angles outside this zone we can expect travel time

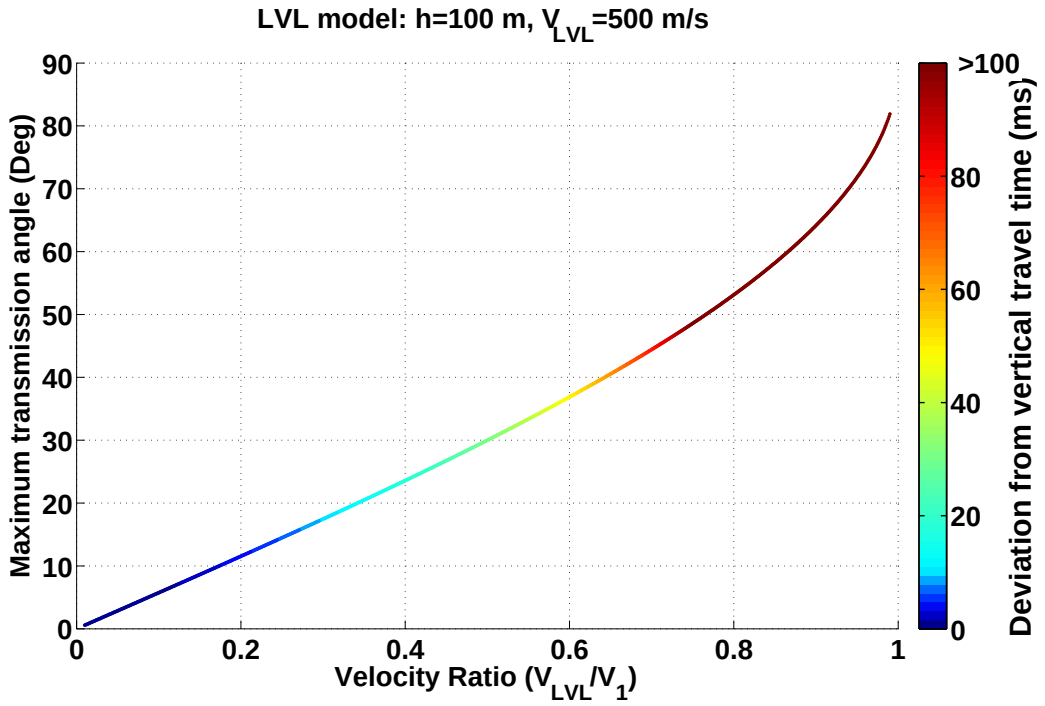

FIG. 2. Maximum transmission angle and relative static increase as a function of the velocity contrast between the LVL and the medium beneath. It is assumed that S-wave velocity decreases when the wavefront is transmitted into the LVL.

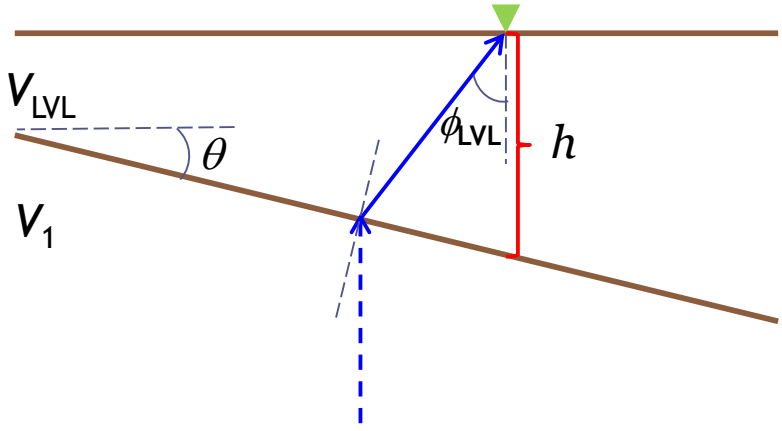

FIG. 3. Geometry used for computing ray-path dependent travel times for a dipping LVL. Here, h is the vertical thickness of the LVL at the receiver location, θ_{LVL} is the ray-path angle in the LVL, ϕ is the dip angle at the base of the LVL, V_{LVL} is the velocity of the LVL and V_1 is the velocity of the underlying medium.

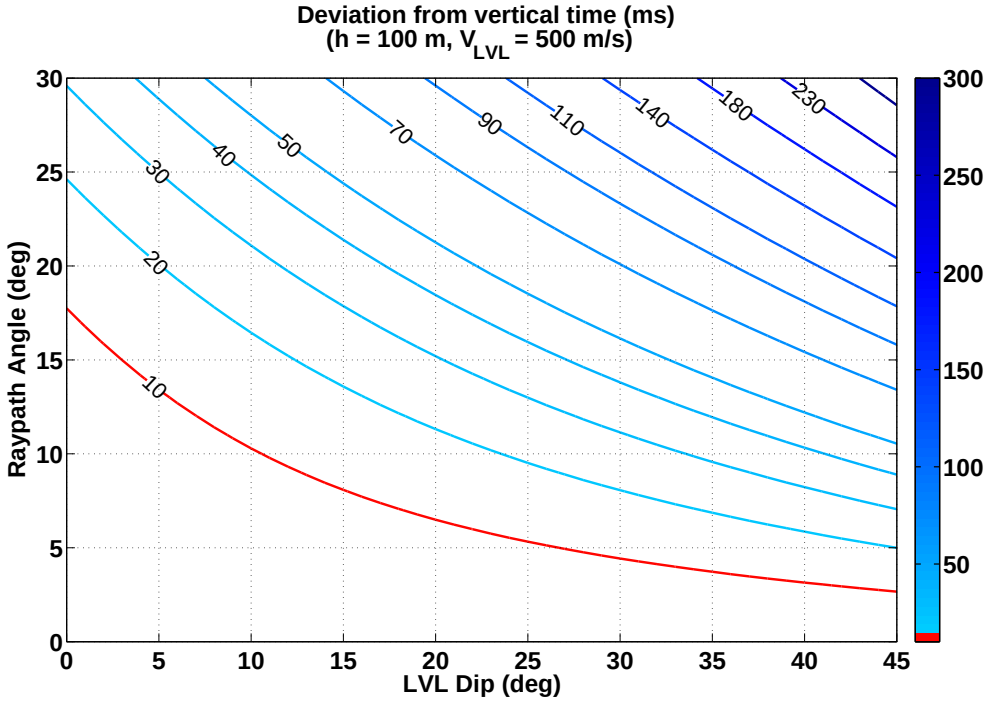

FIG. 4. Expected deviation from the vertical ray-path assumption when changes on the dip of the LVL and the transmission ray-path are considered.

increments in the order of tens of milliseconds when the ray-path angle changes. Under this condition surface consistency is no longer valid. For a fixed receiver location we will need a travel time correction that may change with the ray-path angle. In addition, non-stationarity will arise when the depth of the reflector is considered. This effect is studied in the next section.

Ray Tracing

Figure 5 shows the ray-tracing result for the velocity model at the left. No P-wave velocity contrast was included in the LVL in order to avoid P-wave statics. The colour of each receiver shows the transmission angle of the upgoing rays through the LVL. For the reflector 1, it is possible to identify a change from 0° in the near offsets up to 18° in the far offset. The same change should be observed for a single receiver and several shots. For the deep reflector the range of angles is smaller, with a maximum of 14° at the maximum offset. Since each reflector experienced different transmission angles, the delays suffered by each reflector will be different, even for the same receiver.

In Figure 6 are shown the reflection times for the ray tracing done above. Each reflection time is colored by the transmission angle related to each offset. Results show that reflection times with the same transmission angle, i.e. the same static, are not located at the same offset. The black arrows indicate the lateral shift of reflection times that should have traveled the same distance through the LVL and that should receive the same static correction. Furthermore, for the same offset, i.e. the same receiver location, reflections coming from different depths show different transmission angles, hence they should receive differ-

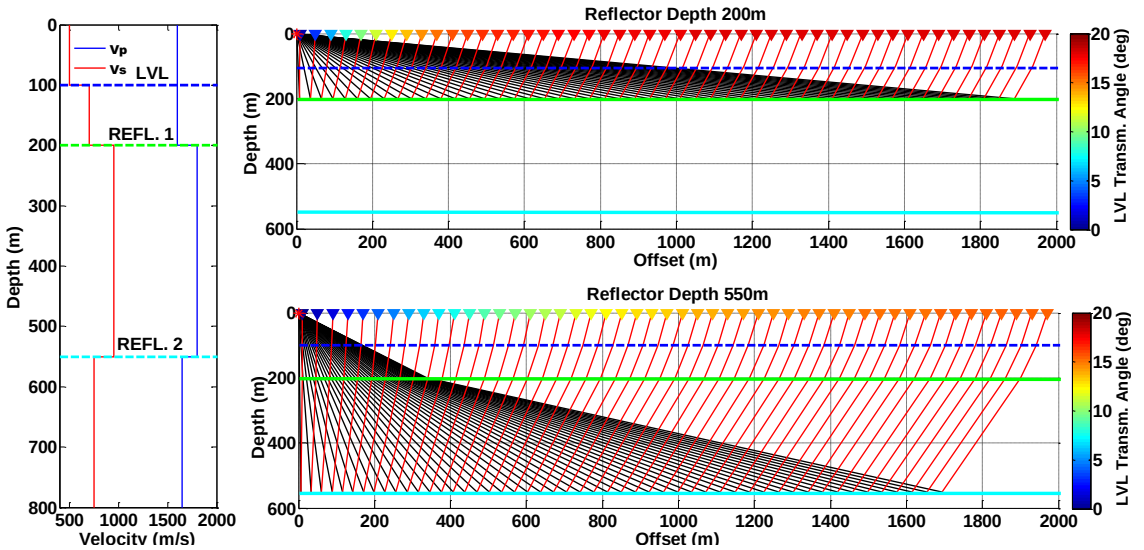

FIG. 5. (left) Velocity model used for ray-tracing. (top) Ray-tracing for the shallow reflector. (bottom) Ray-tracing for the deep reflector. The colour of each receiver represent the transmission angle through the LVL.

ent static correction, implying non-stationary statics. In conclusion, under these conditions non-surface consistency must be taken into account for computing S-wave statics.

In order to address the problem of a dipping LVL and validate the predicted traveltimes given by equation 6, 2D ray-tracing over a gridded model was performed. A low velocity layer with a dip of 45° and velocity of 500 m/s was used for the ray tracing (Figure 7, left). The vertical thickness under the receiver location was set at 50 m. Figure 7 (right) shows a very good match between the travel times given by the analytic formula and those given by the ray tracing. The ray-tracing times display some numerical noise due to the resolution of the gridded model used (1 m).

This match confirms that equation 6 may be used as the engine for the forward modelling of ray-path dependent travel-times. Moreover, matching these travel times with the numerical results for a 2D gridded model also leads us to considerer a tomographic inversion as a plausible tool for building a velocity model for the near surface using ray-path dependent statics.

Finite-Difference Modeling

To address the issue of a structurally complex LVL, finite difference modelling was used for computing synthetic PS-wave shot records. The code used for this modelling was the 2D elastic finite difference code last updated by Manning (2011).

Figure 8 shows the P- and S-wave velocity models used for computing the synthetic data. As in the ray tracing, no changes in P-wave velocity were included in the LVL in order to avoid P-wave statics.

In Figure 9 is shown a raw radial component shot-gather with the most important events

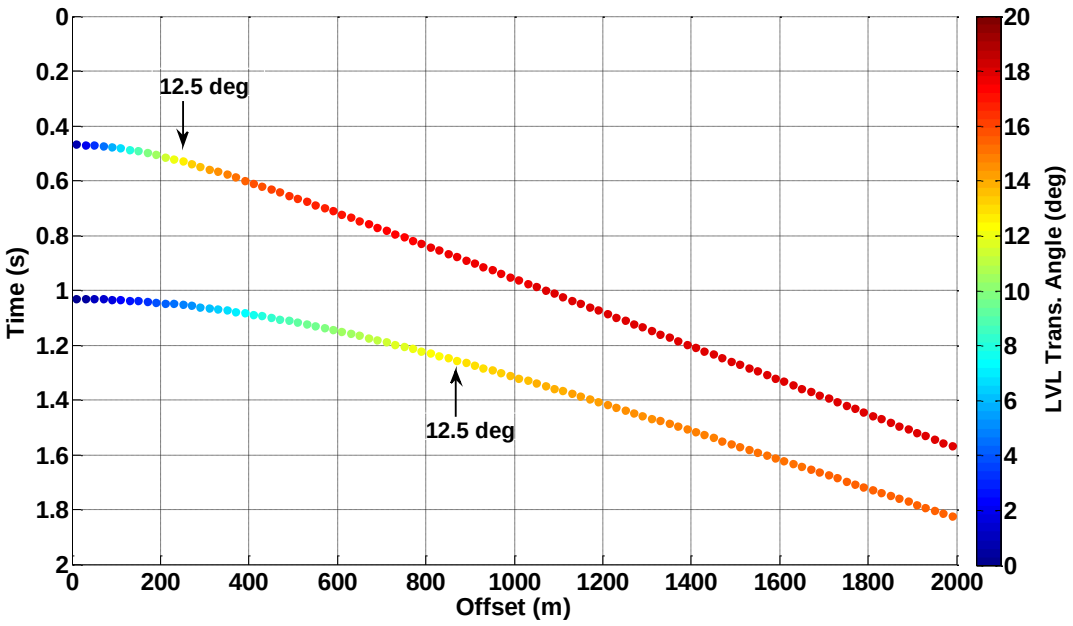

FIG. 6. Angles of transmission for each reflector time given by the ray-tracing. Black arrows indicate how the 12.5° transmission angle is located at different offsets depending on the reflector.

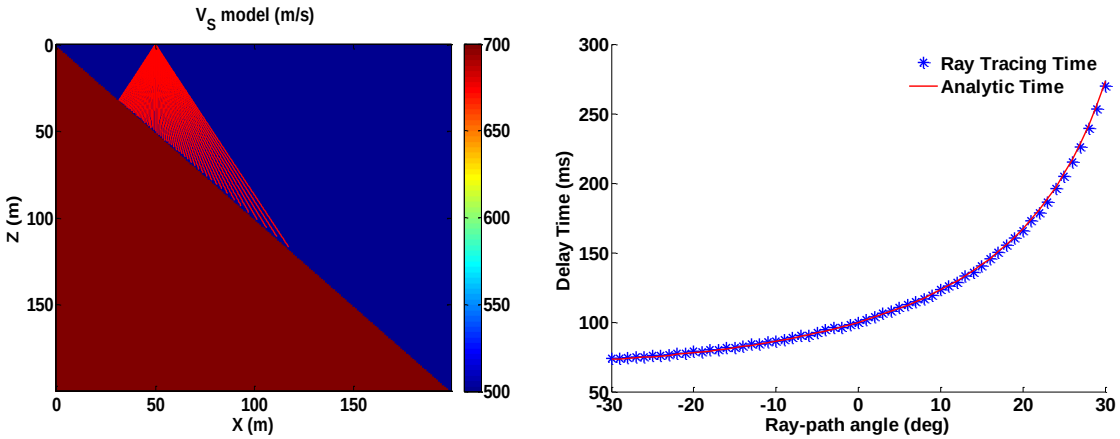

FIG. 7. (left) 2D velocity model with a LVL dipping at 45° used for ray-tracing. In red we can see rays ranging from -30° to 30° respect to the receiver location. (right) Analytic and ray-tracing travel times for a 45° dipping LVL.

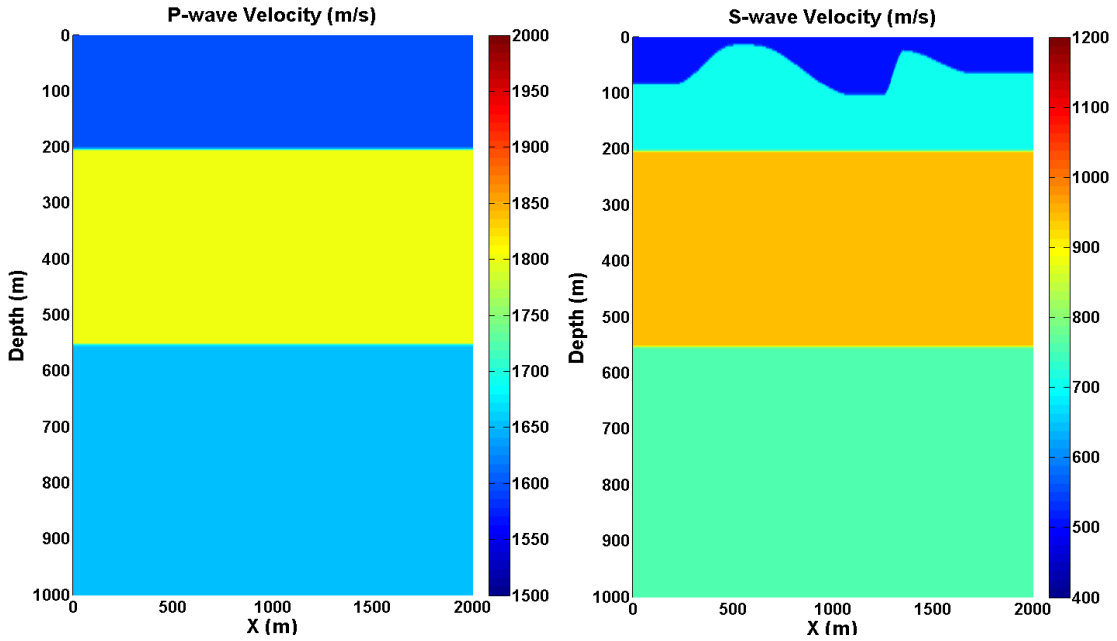

FIG. 8. P-wave (left) and S-wave (rigth) velocity models used for the elastic finite-difference modelling. Notice that there is no LVL in the V_p model and the LVL in the V_s model has been arbitrarily deformed.

identified on the record. Around the 350m offset it is possible to see the effect of the structure of the LVL on the reflections times. The quasi-hyperbolic shape of the PS-reflection has been deformed in a very important way. It is clear that this deformation is being caused by S-wave statics since the P-wave energy projected on the radial component does not display that deformation. Moreover, both reflectors are known to be flat; therefore any delay time other than the moveout of the reflection, must be due to the geometry of the LVL.

To study the non-stationarity of the receiver statics the data were gathered by receiver station and a non-hyperbolic PS-NMO correction (Slotboom, 1990) was applied. Figure 10 shows the receiver gather located at x=1140 m. Although the shallow reflector shows significant residual moveout it is possible to see that there is a shift between traces at similar positive and negative offsets. For the deep reflector the residual moveout effect is less important but there is still a time difference between the reflection times for positive and negative offsets. This problem is an effect of the differences in the structure of the LVL at each side of the receiver.

Figure 11 shows a zoom in the receiver gather 1140 around the two PS-reflectors for the 250 m offset. On this display traces were sorted by absolute offset so negative and positive offsets are now mixed. In Figure 11 (left) it is possible to see that there is a difference of about 22 ms between the reflection travel times for the 250m positive and negative offsets. Furthermore, comparing with the same offset pair for the deep reflector on Figure 11 (right) it is possible to see that the delays are different for each reflector. While the shallow reflector displays a delay of 22 ms, the deep reflector has a 9 ms delay. This effect can be due to the combination of both the structure of the LVL and the difference in the ray-path angle as showed in Figure 6. Applying a constant shift to all the traces of

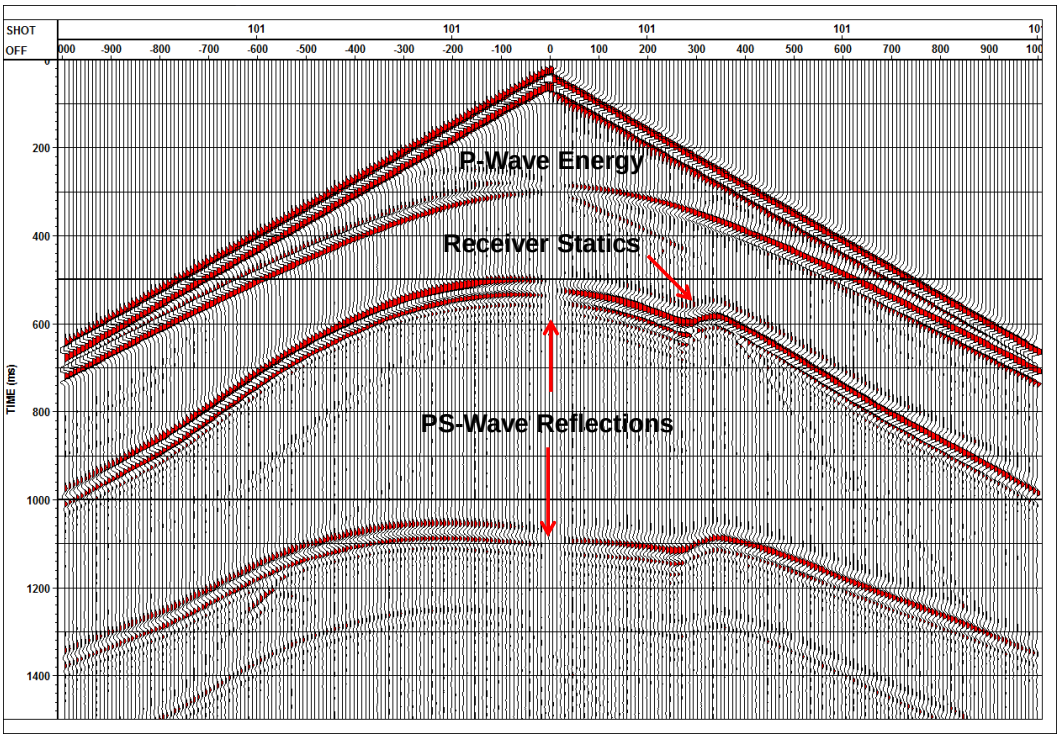

FIG. 9. Raw radial-component gather showing the most important features on the record.

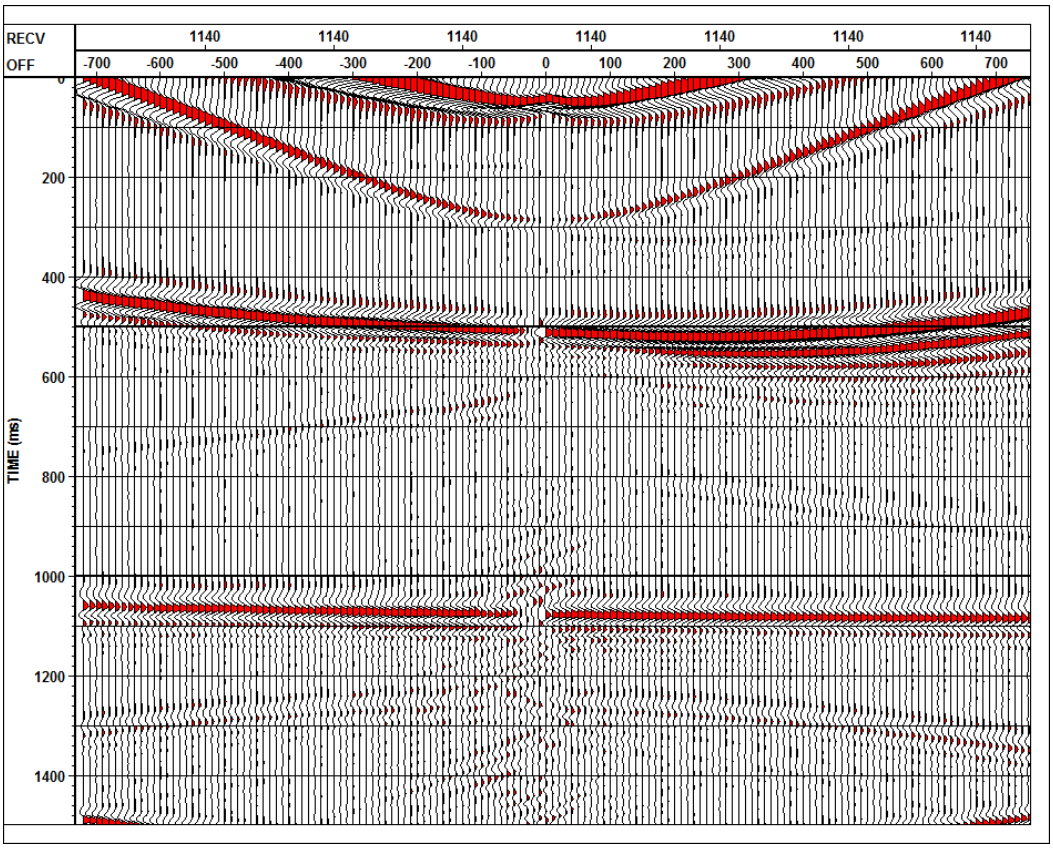

FIG. 10. Receiver gather at station 1140 sorted by signed offset.

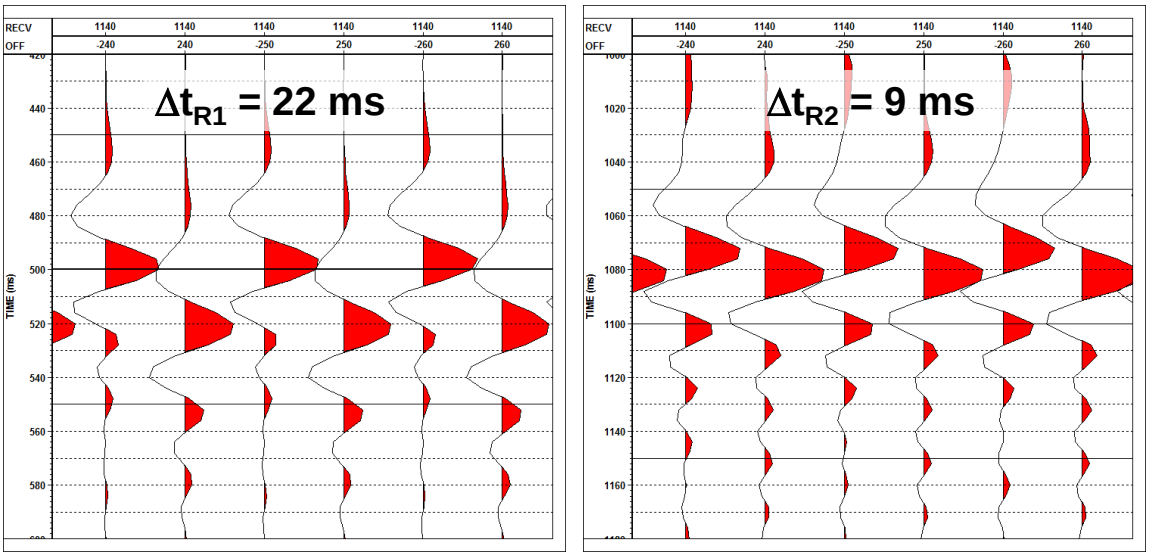

FIG. 11. Difference in the static between traces recorded with negative and positive offsets for the shallow (left) and deep (right) reflectors. Changes in the delay time, at the same offset but for different reflection times, suggest that non-stationary static corrections are needed.

this receiver gather, honoring surface consistency, will deteriorate the stacking power and resolution of one of the reflectors.

Radial Gathers

Since the radial-trace (R-T) transform has the effect of approximately simulating seismic data recorded along straight ray-paths (Henley, 2000), NMO-corrected receiver gathers were transformed to the R-T domain to study the consistency of the statics with the ray-path angle. An exponential gain function and polarity correction were applied to the traces before this process.

Figure 12 shows the output of the R-T transform for receiver gather 1140 sorted by ray parameter value. The term ray parameter, in this context, makes reference to the apparent velocity of the remapping done by the R-T transform. Figure 12 resembles the same characteristics that were described for Figure 10, regarding the residual moveout and the difference in delay times for positive and negative offsets.

In Figure 13 is shown a zoom on Figure 12 around the ray parameter 500 m/s and for the two PS-reflectors. The shifts between consecutive traces, for both reflectors, now display a very close value (ΔtR_1=22 ms and ΔtR_2=20 ms). This result is an evidence that in the ray parameter domain the static value between reflectors is very close. The ability of the radial-trace transform to gather on the same trace reflections with a similar ray parameter leads to a better consistency in the static problem. The remaining shift may be due to the assumption of straight rays made in the application of the radial-trace transform.

Once the static problem is moved to a domain in which the static values can be considered as stationary, computation of the needed corrections can be done in many different ways. In Cova et al. (2013) is explained an interferometric approach for addressing this

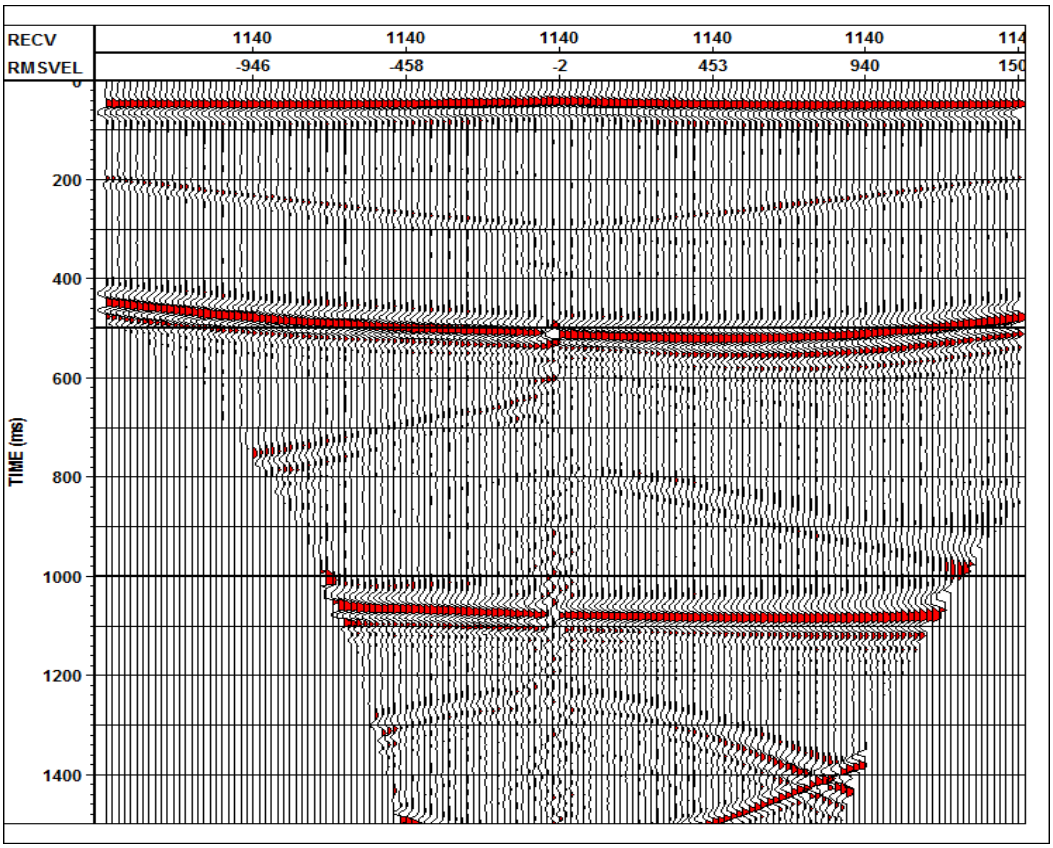

FIG. 12. R-T gather at receiver station 1140 sorted by signed ray parameters

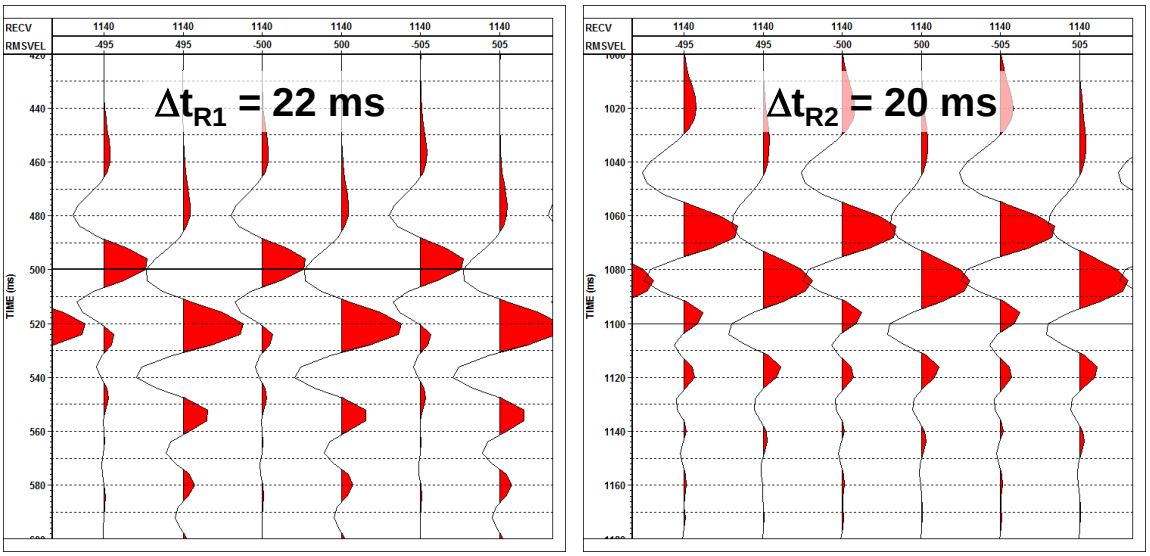

FIG. 13. Delay times between negative and positive ray parameters for the shallow (left) and deep (right) reflectors. Similar static changes on this domain suggest ray-path consistency for the statics corrections.

problem.

SURFACE-CONSISTENT VS RAYPATH-CONSISTENT STACKS

In order to enhance the ray-path dependency of the statics, new synthetic data were computed using a more complex velocity model (Figure 14). The velocity values used in this model are the same than in the flat layers model but we have included different geometries on both reflectors. The reader is referred to Cova et al. (2013) for the details about the processing and computation of ray-path dependent statics for these data. Here we just compare the results of using a surface consistent solution for the statics (Figure 15) versus a ray-path consistent solution (Figure 16). The surface consistent statics were computed using a vertical travel time approximation for each receiver location. Figure 15 shows that the surface consistent solution was not able to correct the static problem for both reflectors simultaneously. At x=1200 m, where the LVL shows a higher dip, the surface consistent solution cannot handle the static problem for either of the reflectors. On the other hand, the stack section on Figure 16 shows a higher level of coherency for both reflectors indicating that the ray-path consistent solution was able to correct the statics problem for both reflectors successfully.

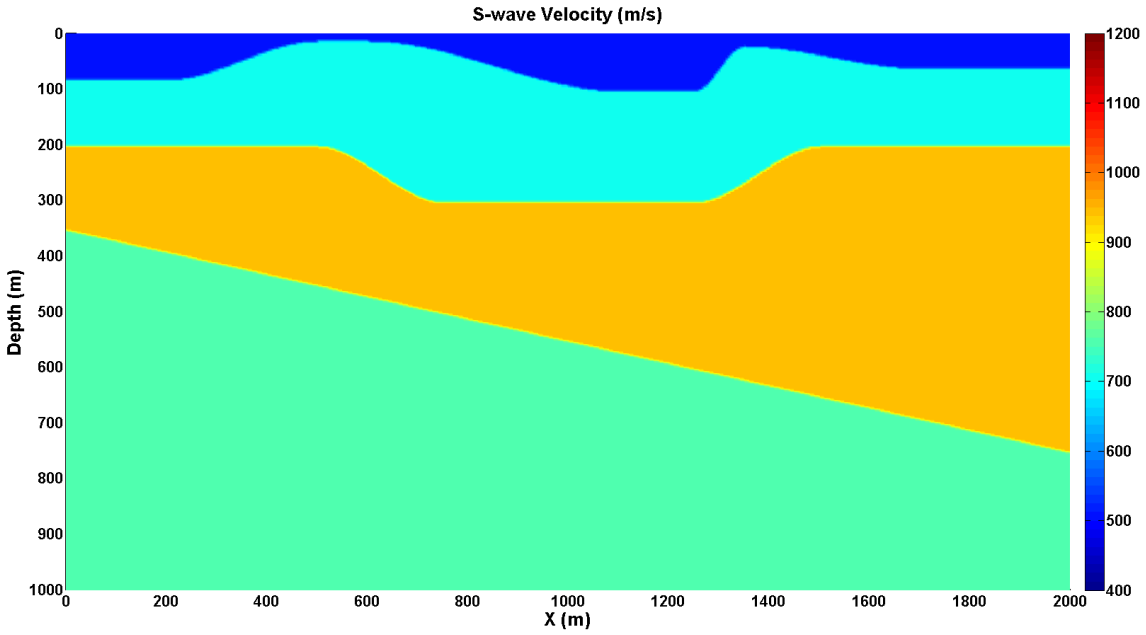

FIG. 14. Velocity model used for computing synthetic data considering a structurally complex LVL and dipping reflectors.

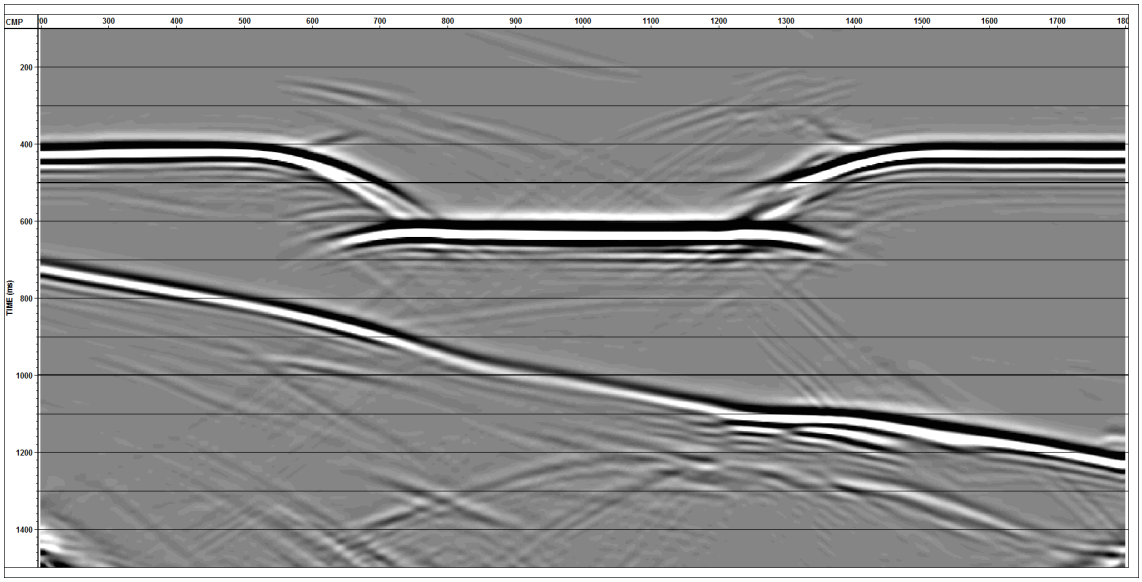

FIG. 15. PS-Stack section after using a surface-consistent solution for the S-wave statics (Cova et al., 2013).

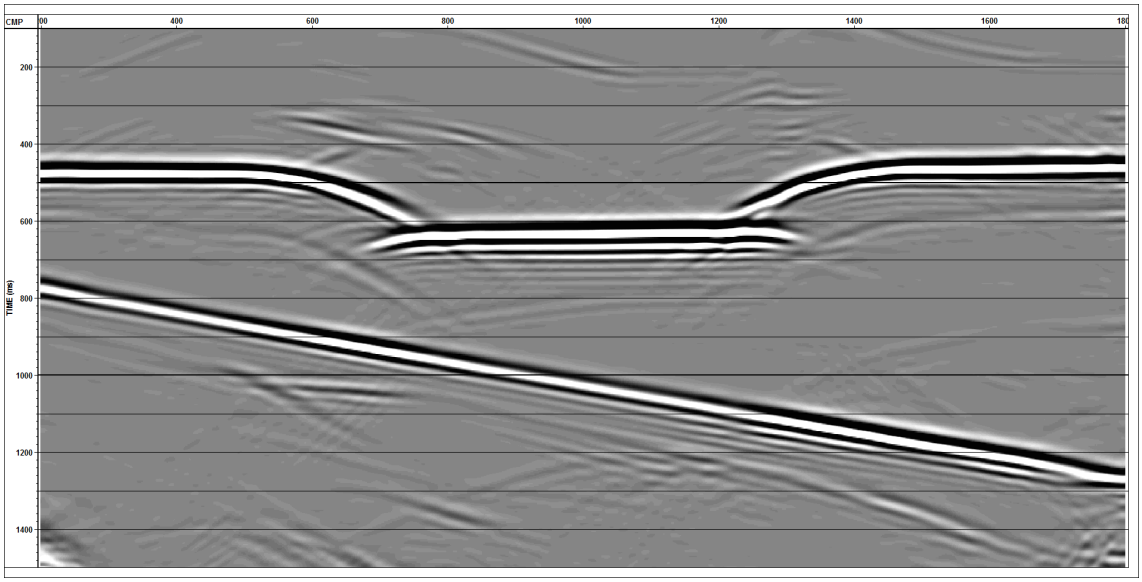

FIG. 16. PS-Stack section after using a raypath-consistent solution for the S-wave statics (Cova et al., 2013).

CONCLUSIONS

Ray trace modelling of PS-raypaths showed how variations in the transmission angle through the LVL can introduce additional static delays. Furthermore, that extra static was found to change with the depth of the reflector, leading to a very clear non-stationarity of the static problem. The magnitude of those changes depend on the velocity contrast between the LVL and the medium beneath it. An additional factor controlling the deviation from the vertical ray-path assumption was the geometry of the LVL.

Synthetic data computed using elastic finite difference modelling showed the effects of the LVL structure on the statics. Dips in the LVL can deviate the ray-paths and change the magnitude of the static depending on the direction of propagation. This also leads to a non-stationary effect. Wavefronts coming from different reflectors can arrive at the same point, at the base of the LVL, with dissimilar angles, leading to different statics correction.

The R-T transform was able to move the static problem to a domain in which they seem to be stationary. This was done by gathering on the same trace reflections that should have traveled with approximately the same ray parameter. Since the R-T transform used here assumes straight ray-paths there are still residual statics that need to be fixed. The Snell ray transform looks to be a very good candidate for improving the effectiveness of the R-T transform for solving non-stationary statics.

As suggested by Equation 6, it is possible to characterize the LVL given a set of ray-path dependent statics for a fixed location. Using this equation for solving the inverse problem is one of the paths that needs to be explored in order to achieve the ultimate goal of computing a S-wave velocity model for the near surface.

ACKNOWLEDGEMENTS

The authors would like to thank to CREWES sponsors for their financial support to this research.

REFERENCES

Cova, R., Henley, D., and Innanen, K., 2013, Interferometric solution for raypath-consistent shear wave statics: CREWES Research Report, **25**.

Henley, D., 2000, More radial trace domain applications: CREWES Research Report, **12**, 21.1–21.14.

Henley, D., 2012, Interferometric application of static corrections: GEOPHYSICS, **77**, No. 1, Q1–Q13.

Manning, P., 2011, Numerical rayleigh wave propagation on a thin layer: CREWES Research Report, **23**, 76.1–76.10.

Slotboom, R. T., 1990, Converted wave (P-SV) moveout estimation: SEG Technical Program Expanded Abstracts, 1104–1106.